Damping estimation from full-scale traffic-induced vibrations of a suspension bridge

Nicolò Daniotti[1,*], Etienne Cheynet[1], Jasna Bogunović Jakobsen[1] and Jonas Snæbjörnsson[1,2]

[1]Department of Mechanical and Structural Engineering and Materials Science, University of Stavanger, N-4036 Stavanger, Norway

[2]School of Science and Engineering, Reykjavik University, Menntavegur 1, 101 Reykjavík, Iceland

[*]*Corresponding author: Nicolò Daniotti,* nicolo.daniotti@uis.no

Abstract

We present an automatic technique for structural damping estimation, based on traffic-induced vibrations of a long-span suspension bridge. First, an identification algorithm is applied to the acceleration data of the Lysefjord bridge to capture traffic load events, i.e. when vehicles are crossing the bridge. Thereafter, time domain decomposition is adopted to compute the modal displacement response triggered by the traffic excitation. The damping ratio and the eigenfrequency are then estimated by fitting a single degree-of-freedom system to the modal response. The damping estimates exhibit a lower dispersion and bias than the corresponding results based on a covariance driven stochastic subspace identification algorithm. In ambient vibration tests, the precision and accuracy of the damping estimates depend on the signal duration. Therefore, it is common to get severely scattered damping values for the low-frequencies modes. Estimating damping ratios using traffic-induced decays removes the problems of frequency resolution for short-length records and may, therefore, complement other ambient vibration techniques.

1 Introduction

Wind and Structural Health Monitoring systems (WASHMS) represent the most reliable tools to assess both the structural and aerodynamic properties of a long-span bridge. Full-scale records are important to validate both numerical models and wind tunnel studies. Damping is a fundamental parameter for the dynamic response of a large wind-sensitive structure. However, its estimation is challenging [1]. The damping estimated from full-scale measurements in long-span bridges is little investigated in the literature due to the inherent problems related to the measurement techniques and the simultaneous participation of different physical phenomena such as hysteresis in the hangers, energy dissipation at supports and expansion joints [2–7]. Even though the structural damping has usually been estimated by taking into account the aerodynamic damping component defined through the quasi-steady theory for turbulent wind loading at different reduced velocities, the stationarity requirement for the wind excitation records is not always mentioned or fully investigated. As already pointed out [4, 5], a non-stationary input signal introduces additional uncertainties, bias and in general an overestimation of the damping ratios [5].

The equivalent viscous damping is commonly adopted to describe the different energy dissipation mechanisms involved in a structural system. The equivalent viscous damping may include aerodynamic damping, friction damping, material damping, and hysteretic damping [4]. For suspension bridges, the main cables may contribute significantly through slippage between the wires (friction damping) [7].

The most common tests applied to estimate the damping of a structure are ambient vibrations, forced vibrations or free vibrations tests. The present work describes an automatic identification technique for the damping ratios based on traffic-induced free vibration decays. The method overcomes the common problems embedded in the frequency domain approaches caused by the increasing probability of non-stationary data for longer records and inadequate frequency resolution in the lower frequency range [4–6, 8]. In fact, the number of discrete frequency steps spanned by the spectral peak is proportional to the ratio between the resonant frequency and the frequency resolution [4, 5]. The methodology used here relies on traffic-induced displacement decays to obtain damping values, in a similar fashion to Rainer

and Van Selst [9], where a controlled vehicle impact was used as an excitation source for all the modes. Assuming that the vibrations modes are sufficiently separated so that the resonant response for each eigen-frequency can be isolated, the damping ratio for each mode is estimated by least square fitting of a SDOF system response to the monitored modal displacement free decay. The low traffic density generally recorded at the Lysefjord bridge and the regular occurrence of heavy vehicles represent the opportunity to develop the aforementioned automated system identification approach. The damping can, therefore, be studied without performing forced resonance tests, which are challenging for long-span bridges. Hence, the method is intended to be complementary to the modal identification techniques previously applied using data from the Lysefjord Bridge [8, 10, 11].

The paper is organized as follows: section 2 describes the Lysefjord Bridge instrumentation, the full-scale input data characteristics and the automatic identification procedures applied to traffic-induced vibrations. Section 3 investigates the damping estimates and the eigenfrequencies, focusing on the complementary characteristics of the method with respect to the ambient vibration analysis.

2 Instrumentation and methods

2.1 The Lysefjord bridge

The Lysefjord suspension bridge is located at the inlet of a narrow fjord in the south-west part of Norway. Its main span is $446\,\mathrm{m}$, with the central part $55\,\mathrm{m}$ above mean sea level and a $12.3\,\mathrm{m}$-wide deck.

Since 2013, the Lysefjord Bridge has been instrumented with a WASHMS, which currently includes nine sonic anemometers and four couples of tri-axial accelerometers located inside the bridge deck. Figure 1 describes the position of the sensors. They are identified through the location of the hangers using the string HXY, where X is the hanger number and Y denotes the west side (W) or east side (E) of the deck. The accelerometers are CUSP-3D from Canterbury Seismic Instruments, with a sampling frequency up to $200\,\mathrm{Hz}$. Considering the frequency range of interest for the present study, the acceleration data are decimated to a sampling frequency of $25\,\mathrm{Hz}$. The sonic anemometers are 3-D WindMaster Pro from Gill instruments, except the one installed on H10W, which is a Weather Transmitter WXT520 from Vaisala. A detail description of the bridge instrumentation can be found in Cheynet et al. [10].

2.2 Full-scale wind velocity and bridge acceleration records

The analysis focuses on low reduced wind velocities $U_{red} = \overline{u}/(Bf)$ (where $\overline{u}$ is the mean wind velocity, B is the deck's width and f is the frequency), for which the response is mostly controlled by the traffic loads and the wind loading effects can be neglected. In addition, low mean wind speeds also reduce the impact of the aerodynamic damping on the total damping and thereby make it possible to evaluate the structural damping. The following results are based on records acquired from July 1, 2017, to June 29, 2018, associated with a mean wind speed lower than $5\,\mathrm{m\,s^{-1}}$ and an along-wind turbulence intensity below 20%. The records are further required to fulfil the first-order flow stationarity conditions, leading to 883 thirty min-long (441.5 hours) acceleration signals. Within this framework, the aerodynamic effects

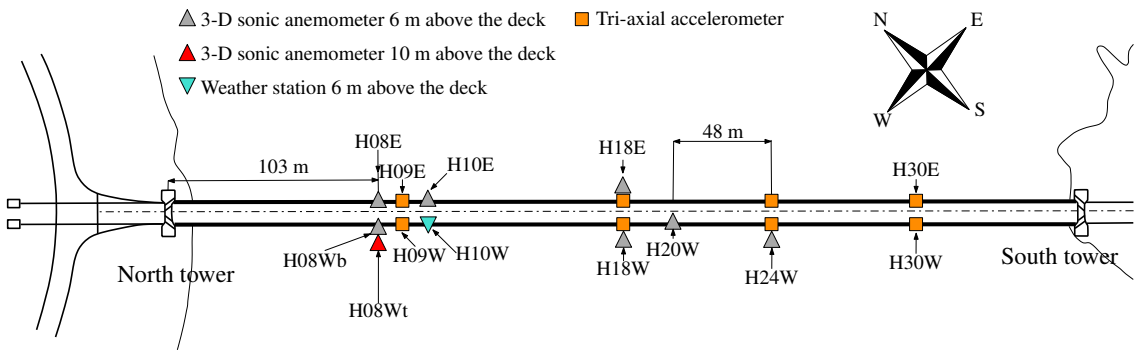

Figure 1. Instrumentation of the Lysefjord bridge since July 2017.

Table 1. Eigenfrequencies of the horizontal, vertical and torsional symmetric and antisymmetric modes of the Lysefjord bridge.

Mode	HS1	HA1	HS2	HA2	HS3	HA3	VS1	VA1	VS2	VA2	VS3	VA3
f_n (Hz)	0.130	0.442	0.556	0.597	0.830	1.000	0.319	0.205	0.439	0.585	0.864	1.194
Mode	TS1	TA1	TS2									
f_n (Hz)	1.215	2.186	3.230									

on the bridge vibrations can be considered negligible when compared to traffic loads.

The present study investigates the modes with eigenfrequencies listed in table 1. The modal analysis is performed using the simplified bridge model described in Cheynet et al. [11]. The modes are identified using the string XYZ, where X=H,V,T represents the lateral (H), vertical (V) and torsional (T) bridge motion, Y=S,A is the symmetric (S) or asymmetric (A) mode shape, and Z is the mode number.

2.3 Damping estimation procedure

The procedure detailed hereafter aims to estimate the damping ratios using traffic as the excitation source. The main idea is to search for the decay signals for each mode of the structure and estimate the corresponding damping, provided that no other vehicles are crossing the bridge and no vehicle enters the bridge for the duration of the analysed decay. Traffic excitation is, therefore, used here in the same way as an impulse load or an imposed displacement is adopted in free vibration tests [12]. In this approach, the identification of the traffic characteristics becomes essential and the knowledge of the vehicles' crossing time is necessary to study the onset of traffic-induced decays.

The enormous amount of acceleration records collected on the Lysefjord Bridge and the low traffic density of the site encourage the use of an algorithm that can automatically detect when a vehicle crosses the bridge. In addition, such an algorithm must be able to evaluate which vehicles can be used as a reliable excitation source for estimating the damping of the bridge. The automatic procedure adopted here can be divided into the following steps: (a) automatic identification of traffic-induced vibrations and onset of displacement decays, which is presented in section 2.4; (b) computation of modal displacements via Time Domain Decomposition (TDD) [13], (c) damping and natural frequency estimation for each considered eigenmode, by fitting an exponentially damped harmonic function to the decay signals.

2.4 Automatic identification of traffic-induced vibrations

The automatic identification procedure is applied to the bridge vertical acceleration response at midspan. The onset of the free decay response is governed by the vehicle departure time, which must thus be estimated as accurately as possible. This is achieved by modeling each vehicle as a moving mass, which is fully described by an arrival time, an equivalent mean speed and an equivalent mass. These parameters are estimated by fitting, in the least-square sense, the computed bridge response induced by a moving mass to the full-scale bridge displacement response. The algorithm can be subdivided into the following steps: (1) the vertical displacements are retrieved based on the acceleration data in the frequency domain; (2) the background response is isolated by means of a high-pass and low-pass zero-phase order 5 digital Butterworth filters, having cut-off frequencies at $0.04\,\mathrm{Hz}$ and $0.15\,\mathrm{Hz}$, respectively. (3) An outlier detection algorithm detects the time instants corresponding to the response peaks caused by traffic [14]. (4) A cluster analysis is used to group together the outliers corresponding to the same identified vehicle. (5) The time instant at which the vehicle enters the bridge main span and its equivalent mean speed are estimated based on the normalized displacement response computed using a "simplified bridge model" [8] and the acquired displacement records. (6) The vehicle mass is eventually estimated in the least-square sense using the non-normalized bridge response.

The outliers detection algorithm is based on the generalized extreme Studentized deviate test [15]. The test version adopted here is able to filter out the lightweight vehicles and multiple vehicles simultaneously crossing the bridge, situations which may mask the target signals we are aiming at. Only clusters having a separation longer than $300\,\mathrm{s}$ are analysed to avoid overlapping of the free decays, especially when considering lower modes, which have a period of vibration up to $7.6\,\mathrm{s}$. Based on the records data described

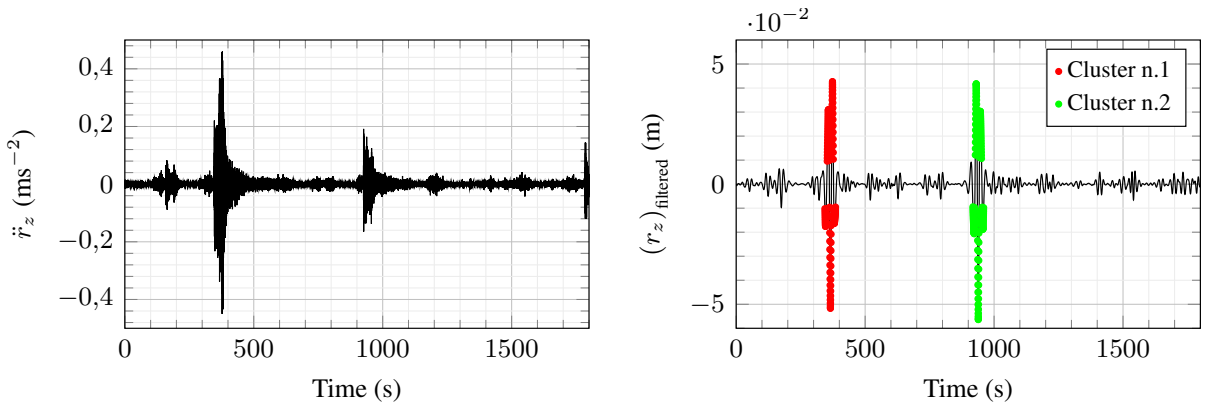

Figure 2. Outliers identification algorithm: acceleration at midspan (left panel); associated filtered displacement response and identified clusters (right panel).

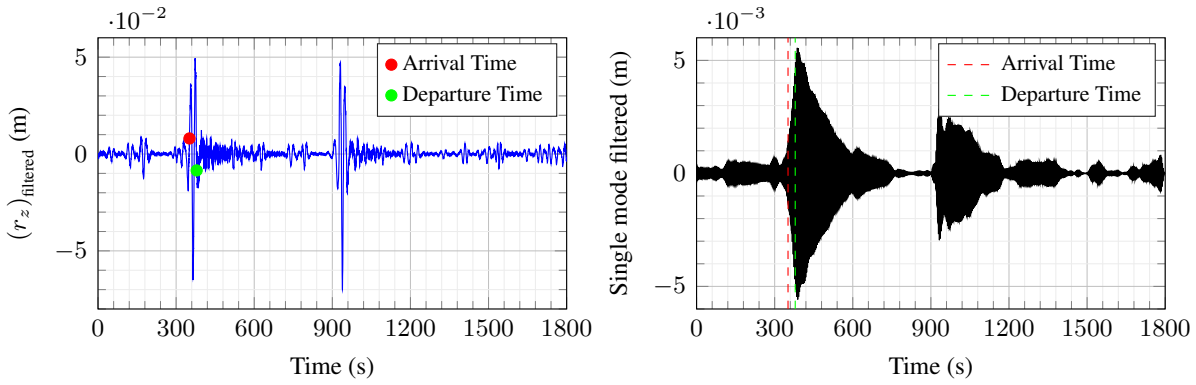

Figure 3. Example of arrival and departure time from the traffic-induced vibrations characterisation: high-pass filtered displacement at midspan (left panel); single-mode VS1 filtered displacement at midpsan (right panel).

in section 2.2, 1284 vehicles are automatically identified. Examples of the aforementioned identification procedure are depicted in figures 2 and 3.

The modal displacement response is computed using the time domain decomposition (TDD) [13], which is appropriate here because the Lysefjord Bridge exhibits well-separated modes. In the present study, all 4 pairs of accelerometers are adopted as input signal sources for the TDD algorithm. The normalised modal displacement, in addition to being the input data for damping estimation, is useful to assess the quality of single-mode filtered and normalised time histories from each sensor.

2.5 Damping estimation

In the present work, the linear viscous damping model is adopted, assuming that it is possible to take into account the different energy dissipation mechanisms involved in the structural system. The free decay response of a SDOF lightly-damped system can be computed as:

$$d(t) = A \cdot e^{-\omega_n \xi t} \cos(\omega_D t + \phi) \tag{1}$$

where $d(t)$ is the target decay signal, starting at peak amplitude A; ω_n is the natural circular frequency; ξ is the damping ratio; $\omega_D = \omega_n \sqrt{1-\xi^2}$ is the damped natural frequency; ϕ is the phase and t is the time. This exponentially damped cosine function (Equation 1) is fitted to the free decay signals described above.

The outcome of the fitting procedure depends on the number of cycles considered within the decay signal. The number of cycles has been chosen as a reference parameter since it allows a consistent comparison of the identified damping ratios for the different modes. When selecting the number of cycles for each mode, a trade-off should be made between the necessity to capture the fully developed decay and

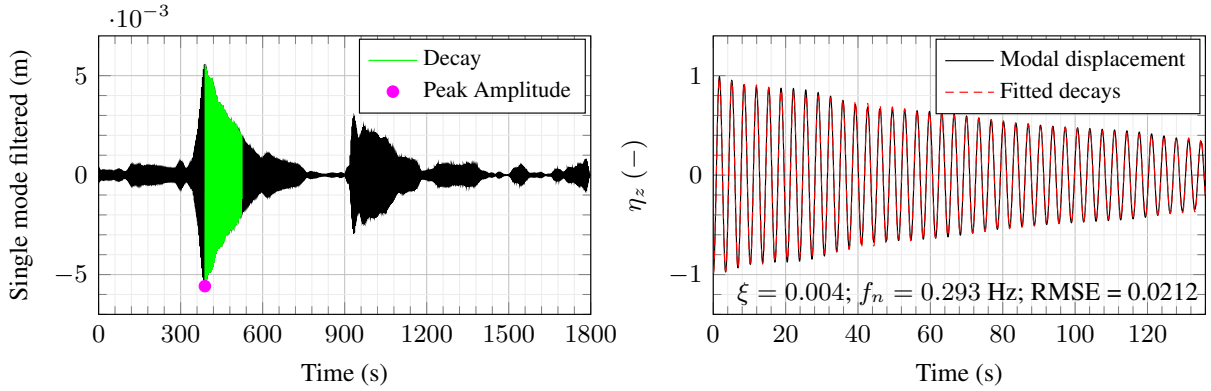

Figure 4. Example of filtered VS1 mode displacement response (left panel), with one window and 40 cycles and corresponding fitted SDOF system (right panel).

the possibility to encounter potential noisy tails. To detect the presence of amplitude-dependent damping ratios, the damping is estimated using a moving rectangular window without overlapping. The absolute maximum within the decay is selected as representative amplitude value and equation 1 is fitted to the windowed normalized modal displacement decay, providing: (1) damping ratio ξ, (2) un-damped natural frequency ω_n and (3) root mean squared error (RMSE), as shown in figure 4.

3 Results

The damping estimates of the Lysefjord Bridge are hereafter presented using their median value ($\widetilde{\xi}$) and standard deviation (σ_ξ). The standard deviation represents the dependency of the modal parameters on the environmental conditions, such as temperature variations or mean wind velocity fluctuations. The probability density functions associated with the damping ratios are not Gaussian, thus the median value is used instead of the arithmetic mean.

The computation of the aerodynamic damping based on the quasi-steady theory for wind loading is not applicable in the present study due to the low wind speed. To account for the dependency of the damping ratios on the mean wind speed, it is possible to establish an empirical relation based on a second-order polynomial fit. However, in the present study, it does not provide a clear relationship for all the modes considered. Nevertheless, the aerodynamic contribution in the estimated damping is found insignificant for mean wind speeds lower than $5\,\mathrm{m\,s^{-1}}$ and the damping ratios considered here are, therefore, assumed to be representative of the structural damping associated with each mode.

As outlined by Xia et al. [16], the natural frequencies of civil structures have a negative correlation with temperature. In the following, the un-damped natural frequency estimates are corrected assuming a linear relationship between the temperature T and the eigenfrequencies f_n. The results are presented in terms of the median value ($\widetilde{f_n}$) and the standard deviation (σ_{f_n}).

No clear dependency was however found in the present study, between the damping ratios and the vibration amplitudes.

To assess the quality of the modal parameter estimates based on traffic-induced decays, the automated covariance driven stochastic subspace identification (SSI-COV) algorithm is applied to all the selected acceleration signals according to the criteria described in section 2.2, all of which have a duration of $30\,\mathrm{min}$. A detailed description of the algorithm can be found in Magalhaes et al. [17], Magalhães and Cunha [18]. In the present study, the adopted time-lags τ for the correlation functions are $15\,\mathrm{s}$, $25\,\mathrm{s}$ and $3\,\mathrm{s}$ for vertical, horizontal and torsional modes, respectively. Such values correspond to 3 or 4 times the largest eigen-periods, which is consistent with the time-lag values used by Brownjohn et al. [19] and Magalhaes et al. [17].

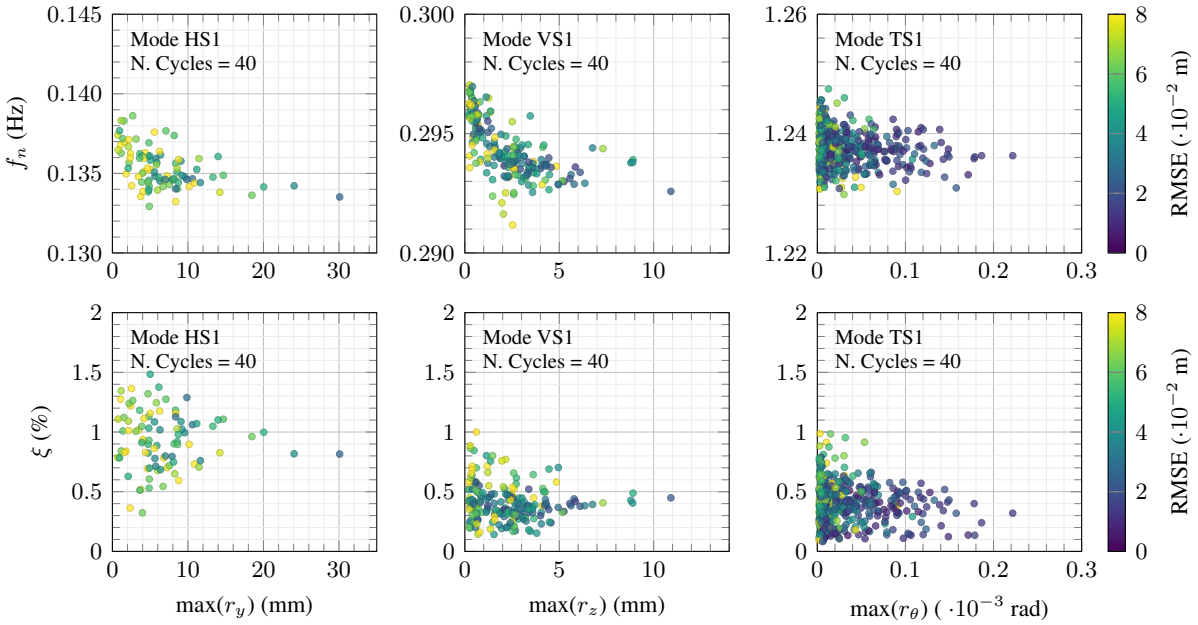

Figure 5. Estimation of natural frequencies f_n and damping ratios ξ for the HS1, VS1 and TS1 modes.

3.1 Damping ratio based on traffic-induced decays

A single window of 40 cycles starting from the maximum of the response (within the first cycles after the departure time) is adopted for the damping estimation. Within each decay time series, about forty cycles represent an effective candidate for the damping estimation, providing a good trade-off between decay fitting quality, minimisation of standard deviation and number of reliable outcomes. To reduce the influence of outliers on the statistical representation of the damping and enhance the quality of the analysed signals, we focus on values below the 95^{th} percentile only. The estimates of the damping ratios and un-damped natural frequencies for the HS1, VS1 and TS1 modes are depicted in figure 5 as an example. The median value and the standard deviation of the estimated damping ratios, as well as the corresponding natural frequencies for all the considered modes are reported in table 2. In the following, the quantity $x \pm y$ stands for median value $\pm$ standard deviation.

The damping ratios for vertical and torsional modes are, as expected for a steel welded box-girder suspension bridge, low, or in the range $\xi \simeq 0.3 - 0.5\%$, as suggested by Larsen and Larose [3]. The damping of HS1 mode is $0.92\% \pm 0.22$, which is in overall agreement with the median value 0.80% estimated in Cheynet et al. [8] with the automated SSI-COV algorithm [8, 17]. The HS2 and HA2 modes exhibit low median damping values, of 0.17% and 0.16% respectively. A modal analysis from a finite element model of the Lysefjord bridge [20] shows that for such modes, the main cables are characterised by larger vibration amplitude than the deck. Consequently, a lower mass participation factors of the deck may suggest that the damping mechanisms associated with the deck and joints are inactive for these vibration modes. The median damping estimates are in general agreement with full-scale observations on long-span bridges available in Simiu and Miyata [2] and the corresponding standard deviations are lower than 0.22% for all the modes considered. Such a low scatter is achieved by automatically addressing high-quality single-mode decays with stationary input data and pre-identified traffic load scenarios.

The damping ratios studied here do not follow the inverse proportionality between damping and natural frequency, which is generally observed for long-span suspension bridges [7]. However, it should be noted that many full-scale wind velocity observations may not verify the assumption of flow stationarity, the validity of which decreases for records of longer duration. In addition, it is well known that frequency-domain-based system identification methods may overestimate the damping ratios due to the intrinsic lower frequency resolution for the lower frequency modes [4, 5, 21].

The modal parameters estimated using the automated SSI-COV algorithm applied to the $30\,\mathrm{min}$ long displacement time-series are also reported in table 2. The median value and the dispersion of damping

Table 2. Median value and standard deviation of the identified damping ratios ξ and un-damped natural frequencies f_n: comparison between the traffic-induced decays method and the automated SSI-COV algorithm.

	Traffic-induced decays				SSI-COV			
Mode	$\widetilde{f_n}$	σ_{f_n}	$\widetilde{\xi} \cdot 10^{-2}$	$\sigma_\xi \cdot 10^{-2}$	$\widetilde{f_n}$	σ_{f_n}	$\widetilde{\xi} \cdot 10^{-2}$	$\sigma_\xi \cdot 10^{-2}$
VS1	0.294	0.001	0.38	0.13	0.295	0.001	0.42	0.15
VS2	0.408	0.003	0.36	0.15	0.410	0.003	0.56	0.18
VS3	0.852	0.002	0.41	0.15	0.853	0.004	0.52	0.19
VA1	0.221	0.002	0.31	0.15	0.223	0.002	0.68	0.17
VA2	0.586	0.003	0.39	0.15	0.588	0.003	0.50	0.19
VA3	1.165	0.005	0.52	0.17	1.162	0.005	0.68	0.26
HS1	0.135	0.001	0.92	0.22	0.136	0.001	1.12	0.27
HS2	0.577	0.001	0.17	0.05	0.574	0.001	0.13	0.06
HS3	0.860	0.005	0.68	0.22	0.867	0.007	0.65	0.34
HA1	0.443	0.004	0.61	0.13	0.445	0.004	0.78	0.20
HA2	0.625	0.001	0.16	0.06	0.626	0.001	0.15	0.08
HA3	1.012	0.009	0.54	0.17	1.013	0.009	0.83	0.37
TS1	1.238	0.003	0.39	0.13	1.236	0.005	0.54	0.29
TS2	3.219	0.010	0.41	0.13	3.216	0.014	0.57	0.15
TA1	2.183	0.006	0.45	0.12	2.177	0.012	1.01	0.37

ratios estimated are, as expected, larger than the ones computed by means of traffic-induced modal vibration decay fitting. Hence the results based on traffic-induced vibration decay fitting are considered more accurate. In fact, results based on ambient vibration tests usually show a rather high bias, mainly due to the finite length of records, the variation of the environmental conditions and variability in the loading characteristics. Most of the median value obtained from traffic-induced vibrations lie within the range defined by median $\pm$ standard deviation of the damping ratios estimated using the automated SSI-COV algorithm, thereby validating in this way the goodness of the proposed methodology. Finally, it can be noted that damping estimates for the modes HS2 and HA2, based on the automated SSI-COV algorithm, agree with the low values previously mentioned for the modes HS2 and HA2.

4 Conclusions

An automatic identification procedure for estimation of the damping ratios of long-span suspension bridges based on traffic-induced vibration decay is proposed and implemented for the Lysefjord bridge. The input records rely on stationary flow conditions with mean wind speed below $5\,\mathrm{m\,s^{-1}}$ to minimise the impact of the aerodynamic damping and better address the bridge response induced by traffic. An algorithm identifying outliers coupled with a cluster analysis method is applied to automatically characterise traffic-induced vibrations, namely to identify when vehicles cross the bridge. The modal displacements are retrieved via Time Domain Decomposition and the onset of traffic-induced displacement decay is identified for each mode. The damping ratios and un-damped natural frequencies are estimated by fitting an exponentially damped sinusoid function to the decay signal, in the same fashion as done in traditional free-decay testing. Because the damping ratios of the low-frequency modes are estimated more accurately by this method than by the automated covariance driven stochastic subspace identification algorithm, the proposed procedure may be coupled with classical system identification techniques to study the damping ratios of a long-span bridge.

Acknowledgements

The support of the Norwegian Public Roads Administration to the monitoring project on the Lysefjord bridge is gratefully acknowledged.

References

[1] Kareem, A., Gurley, K.. Damping in structures: its evaluation and treatment of uncertainty. Journal of Wind Engineering and Industrial Aerodynamics 1996;59(2-3):131–157.

[2] Simiu, E., Miyata, T.. Design of buildings and bridges for wind: a practical guide for ASCE-7 standard users and designers of special structures. 2006.

[3] Larsen, A., Larose, G.L.. Dynamic wind effects on suspension and cable-stayed bridges. Journal of Sound and Vibration 2015;334:2–28.

[4] Brownjohn, J.. Estimation of damping in suspension bridges. Proceedings of the Institution of Civil Engineers - Structures and Buildings 1994;104:401–415.

[5] Brownjohn, J., Dumanoglu, A., Severn, R., Taylor, C.. Ambient vibration measurements of the Humber suspension bridge and comparison with calculated characteristics. Proc of the Institution of Civil Engineers (London) 1987;83:561–600.

[6] Brownjohn, J., Bocciolone, M., Curami, A., Falco, M., Zasso, A.. Humber bridge full-scale measurement campaigns 1990–1991. Journal of Wind Engineering and Industrial Aerodynamics 1994;52:185–218.

[7] Davenport, A., Larose, G.L.. The structural damping of long span bridges, and interpretation of observations. In: Canada-Japan Workshop on Bridge Aerodynamics, Ottawa. 1989,.

[8] Cheynet, E., Jakobsen, J.B., Snæbjörnsson, J.. Damping estimation of large wind-sensitive structures. Procedia engineering 2017;199:2047–2053.

[9] Rainer, J., Van Selst, A.. Dynamic properties of Lions gate suspension bridge. ASCE/EMD Specialty Conference 1976;:243–252.

[10] Cheynet, E., Jakobsen, J.B., Snæbjörnsson, J.. Buffeting response of a suspension bridge in complex terrain. Engineering Structures 2016;128:474–487.

[11] Cheynet, E., Snæbjörnsson, J., Jakobsen, J.B.. Temperature effects on the modal properties of a suspension bridge. In: Dynamics of Civil Structures, Volume 2. Springer; 2017, p. 87–93.

[12] Magalhães, F., Cunha, Á., Caetano, E., Brincker, R.. Damping estimation using free decays and ambient vibration tests. Mechanical Systems and Signal Processing 2010;24(5):1274–1290.

[13] Kim, B.H., Stubbs, N., Park, T.. A new method to extract modal parameters using output-only responses. Journal of sound and vibration 2005;282(1-2):215–230.

[14] Cheynet, E., Snæbjörnsson, J., Jakobsen, J.B.. Identifying traffic-induced vibrations of a suspension bridge: A modelling approach based on full-scale data. In: International Modal Analysis Conference (IMAC) 37th, January 28-31, 2019, Orlando, Florida. 2019,.

[15] Rosner, B.. Percentage points for a generalized ESD many-outlier procedure. Technometrics 1983;25(2):165–172.

[16] Xia, Y., Chen, B., Weng, S., Ni, Y.Q., Xu, Y.L.. Temperature effect on vibration properties of civil structures: a literature review and case studies. Journal of civil structural health monitoring 2012;2(1):29–46.

[17] Magalhaes, F., Cunha, A., Caetano, E.. Online automatic identification of the modal parameters of a long span arch bridge. Mechanical Systems and Signal Processing 2009;23(2):316–329.

[18] Magalhães, F., Cunha, A.. Explaining operational modal analysis with data from an arch bridge. Mechanical systems and signal processing 2011;25(5):1431–1450.

[19] Brownjohn, J., Magalhaes, F., Caetano, E., Cunha, A.. Ambient vibration re-testing and operational modal analysis of the Humber bridge. Engineering Structures 2010;32(8):2003–2018.

[20] Wang, J., Cheynet, E., Jakobsen, J.B., Snæbjörnsson, J.. Time-domain analysis of wind-induced response of a suspension bridge in comparison with the full-scale measurements. In: ASME 2017 36th International Conference on Ocean, Offshore and Arctic Engineering. 2017,.

[21] Jones, N.P., Spartz, C.A.. Structural damping estimation for long-span bridges. Journal of engineering mechanics 1990;116(11):2414–2433.